EUROPEAN ORGANIZATION FOR NUCLEAR RESEARCH

CERN-EP/84-114
3 September 1984

PS184: A STUDY OF $\bar{p}$-NUCLEUS INTERACTION WITH A HIGH-RESOLUTION MAGNETIC SPECTROMETER

D. Garreta, P. Birien, G. Bruge, A. Chaumeaux, D.M. Drake*), S. Janouin, D. Legrand, M.C. Lemaire, B. Mayer, J. Pain and J.C. Peng*)

DPHN/ME, CEN, Saclay, France

M. Berrada, J.P. Bocquet, E. Monnand, J. Mougey and P. Perrin

DRF, CEN, Grenoble, France

E. Aslanides and O. Bing

CRN, Strasbourg, France

A. Erell, J. Lichtenstadt and A.I. Yavin

Tel Aviv University**), Tel Aviv, Israel

(Presented by D. Garreta)

Contribution to the
7th European Symposium on Antiproton Interactions
Durham, United kingdom, 9–13 July 1984

---

*) Permanent address: Los Alamos National Laboratory, New Mexico, USA. Supported in part by the US Department of Energy.

**) Supported by the Israel Fund for Basic Research.

PS184: A STUDY OF $\bar{p}$–NUCLEUS INTERACTION WITH A HIGH-RESOLUTION MAGNETIC SPECTROMETER

D. Garreta, P. Birien, G. Bruge, A. Chaumeaux, D.M. Drake*), S. Janouin, D. Legrand, M.C. Lemaire, B. Mayer, J. Pain and J.C. Peng*)

DPHN/ME, CEN, Saclay, France

M. Berrada, J.P. Bocquet, E. Monnand, J. Mougey and P. Perrin

DRF, CEN, Grenoble, France

E. Aslanides and O. Bing

CRN, Strasbourg, France

A. Erell, J. Lichtenstadt and A.I. Yavin

Tel Aviv University**), Tel Aviv, Israel

Abstract. The aim of the experiment PS184 at LEAR is to study a few simple and well-defined channels of the $\bar{p}$–nucleus interaction using SPES II, a high-resolution magnetic spectrometer with large solid angle and momentum acceptances [Thirion and Birien]. Results of elastic scattering from ^{12}C, ^{40}Ca and ^{208}Pb, inelastic scattering from ^{12}C, and $(\bar{p},p)$ knock-out reaction from ^{12}C, ^{63}Cu and ^{209}Bi, are presented. An optical-model analysis of the elastic-scattering data as well as microscopic KMT-type calculations have been performed.

1. INTRODUCTION

Before the advent of LEAR in 1983 very little was known about the $\bar{p}$–nucleus interaction at low energy. From the experimental point of view the data were scarce and of rather poor quality, consisting mainly of bubble-chamber data [Agnew et al., 1957], a few reaction cross-sections [Aihara et al., 1981] and level widths and shifts from X-ray studies of antiprotonic atoms [Batty, 1981]. The analysis of these data yielded non-unique $\bar{p}$–nucleus optical potentials [Wong et al., 1984] leading to elastic scattering angular distributions [MacKellar et al., 1984] with very different behaviours at sufficiently large angles (see Fig. 1). From the theoretical point of view very large ambiguities also existed which were leading to $\bar{p}$–nucleus optical potentials with a real part ranging from strongly attractive to repulsive values [Bouyssy and Marcos, 1982; Auerbach et al., 1981; Niskanen and Green, 1983]. Therefore, the main purpose of the elastic-scattering measurements (which, in contrast with other recent measurements [Nakamura et al., 1984; Sakitt, 1984], cover a wide angular range and have elastically scattered antiprotons well resolved, with no pion contamination) was to set constraints on the $\bar{p}$–nucleus potential. This would in particular supply some information on the possibility of $n\bar{n}$ oscillations [Dover et al., 1983]. Using microscopic calculations they may also provide a test of the elementary $\bar{N}N$ amplitudes. Inelastic scattering from collective states also sets constraints on the $\bar{p}$–nucleus potential when analysed in terms of coupled channel calculations. When unnatural parity states are concerned it provides a sensitive test of the spin and isospin components of the $\bar{N}N$ elementary amplitudes [Dover et al., 1984]. The purpose of the $(\bar{p},p)$ knock-out reaction was to observe possible bound or resonant states of an antiproton and a nucleus which would be formed in a way similar to that of the (K^-, π) "recoilless" hypernuclei production. The width of such states is predicted to be very large [Green and Wyceh, 1982; Wong et al., 1984] but their observation, speculative as it might be, would provide very useful information on the inner part of the $\bar{p}$–nucleus potential.

*) Permanent address: Los Alamos National Laboratory, New Mexico, USA. Supported in part by the US Department of Energy.

**) Supported by the Israel Fund for Basic Research.

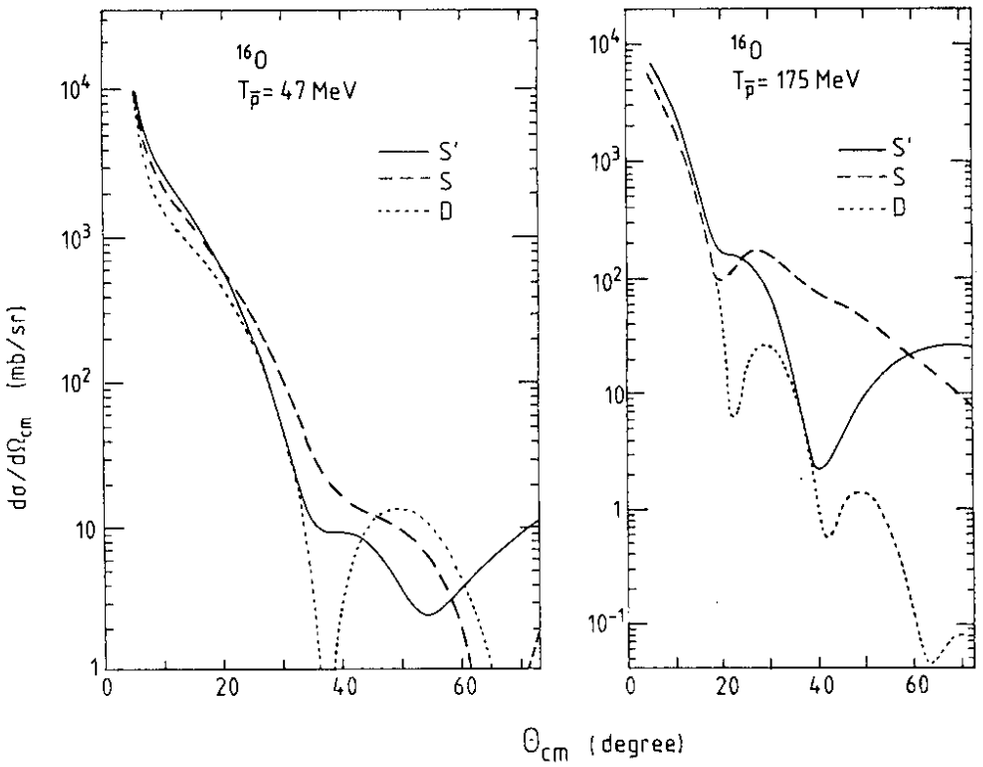

Fig. 1 $\bar{p}$ + ^{16}O elastic scattering angular distributions calculated with S-type (S and S') and D-type (D) optical potentials of MacKellar et al. [1984].

2. EXPERIMENTAL SET-UP (See Fig. 2)

The incident antiprotons (with an intensity ranging from 2×10^4 to 10^5/s) were counted by a 0.36 mm thick scintillation (S_1) located 25 cm in front of the target. Scattered antiprotons, or outgoing protons, were momentum analysed in the magnetic spectrometer SPES II, which has a momentum resolution of 5×10^{-4}, a solid angle of 30 msr and a momentum acceptance of ±18%. They were detected in three multiwire proportional chambers (MWPCs) [Chaminade et al., 1974] and a scintillator hodoscope located near the focal plane. Pions produced by annihilation in the target were discarded by time-of-flight measurement. Information from the MWPCs was used to compute the scatttering angle and the excitation energy of the residual nucleus. For elastic and inelastic scattering the full angular acceptance was divided into 1.67° bins. The energy resolution was about 1 MeV (FWHM) and the overall angular resolution, including multiple scattering in the target, varied from about 2° for the C and Ca targets to about 3° for the Pb target. The uncertainty on the absolute scattering angle was 0.2°. The uncertainty on the absolute normalization is 10%.

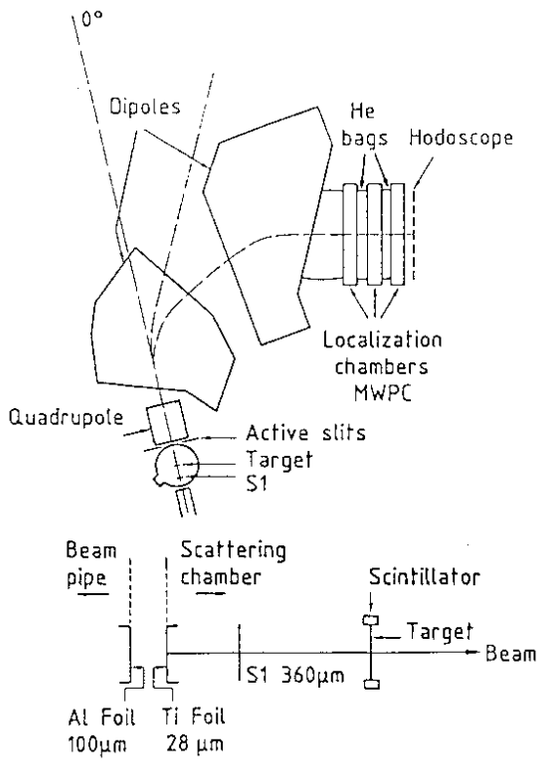

Fig. 2 PS184 experimental set-up.SPES II is represented at 0° scattering angle.

3. ELASTIC SCATTERING

Angular distributions of antiproton elastic scattering are shown in Fig. 3 for ^{12}C at 46.8 MeV [Garreta et al., 1984a] and in Fig. 4 for ^{12}C, ^{40}Ca, and ^{208}Pb at 180 MeV [Bruge, 1984; Garreta et al., 1984b] (solid dots). One can immediately see that they exhibit oscillatory behaviour typical of a diffraction pattern, similar to that

calculated with a D-type potential shown in Fig. 1 and very different, at sufficiently large angle, from that corresponding to an S-type potential or that of proton elastic scattering (open circles) also shown for comparison. This agreement between our data and strongly absorptive potential predictions is confirmed by an optical-model analysis performed using the ECIS code of Raynal [1981] with an optical potential parametrized by a Woods-Saxon geometry, with volume absorption and with no spin orbit, typical examples of which are shown as solid curves in Figs. 3 and 4. Although equally good fits were achieved with optical potentials having quite different geometries, they all had similar values V(R) and W(R) (shown in Table 1) at a distance R, radius of strong absorption [Barrett and Jackson, 1977], and are all strongly absorbing, that is $|W(R)| \gtrsim 2|V(R)|$. This indicates that a necessary condition for orbiting does not exist [Auerbach et al., 1981; Kahana and Sainio, 1984]. When the geometrical parameters of the real and imaginary parts are assumed to follow those of the point charge distribution, corrected for the interaction range, taken as a Yukawa function with $\mu^{-1} = 0.6$ fm, V_0 and W_0 become well determined. These values are also shown in Table 1, where we can see that $V_0 < 70$ MeV

Table 1

Real and imaginary potentials at the radius of the strong absorption and calculated reaction cross-sections. Also shown are the strengths of the real and imaginary potentials obtained by using a geometry derived from that of the charge distribution (see text).

Target	$E_{\bar{p}}$ (MeV)	R (fm)	V(R) (MeV)	W(R) (MeV)	σ_R (mb)	V_0 (MeV)	W_0 (MeV)
^{12}C	46.8	3.7	-3.5 ± 1.5	-8.5 ± 1	600 ± 30	35 ± 4	77 ± 4
^{12}C	179.7	3.3	-7.8 ± 1.5	-19.6 ± 2	500 ± 25	44 ± 4	96 ± 2
^{40}Ca	179.8	4.94	-6.2 ± 1.5	-13.3 ± 2	990 ± 50	43 ± 4	119 ± 3
^{208}Pb	180.3	8.15	-5.4 ± 1.5	-10.2 ± 2	2670 ± 140	60 ± 6	152 ± 2

and $W_0 \gtrsim 2\,V_0$. These results remove the ambiguity [Wong, 1984] in the $\bar{p}$–nucleus interaction, by rejecting the shallow (S-type) imaginary potentials. Moreover, the depth V_0, which for ^{12}C does not show the strong energy dependence predicted by some models [Bouyssy and Marcos, 1982; Niskanen and Green, 1983], is shallower than that calculated in the relativistic mean-field approach [Bouyssy and Marcos, 1982], and provides a lower limit for the $n\bar{n}$ oscillation time [Dover et al., 1983], $\tau_{\bar{n}n}$, of about 3×10^7 s. Despite the optical-model ambiguities, the reaction cross-sections are well determined in the present analysis, and their values are given in Table 1. The decrease with incident energy of both R and σ_R, as seen in the table, is consistent with the energy dependence of the $\bar{p}N$ cross-section. At 180 MeV the reaction cross-section can be represented by the expression $\sigma_R = \pi (a + r_0 A^{1/3})^2$, with $a \simeq 0.65$ fm and $r_0 \simeq 1.44$ fm. Our determination of σ_R for ^{12}C agrees with that of Nakamura et al. [1984], whereas the value quoted by Aihara et al. [1981] is 20% lower.

Results of microscopic calculations are also shown in Figs. 3 and 4. The dashed and dotted curves represent KMT-type calculations done with the $\bar{p}N$ amplitudes of Dover and Richard [1982] or of the Paris potential [Coté et al., 1982], respectively. The proton density was taken from electron-scattering analysis and the neutron density from scattering of high-energy protons and kaons. Both predictions, which have no free parameters, agree with the data reasonably well. This agreement is somewhat surprising in view of the necessary conditions for KMT calculations to be valid. We note that a recent Glauber-type calculation [Dalkarov and Karmanov, 1984], also agrees with the data at 46.8 MeV. A possible explanation for these agreements is that the elementary $\bar{p}N$ scattering is forward peaked, a condition favourable to multiple-scattering calculations. Our results also agree with the predictions of von Geramb et al. [1984] (not shown), whose method was originally developed for nucleon–nucleus scattering with the nuclear matter approach [von Geramb, 1979]. The agreement of the prediction by Niskanen and Green [1983] with the 46.8 MeV data all but disappears at 180 MeV [Niskanen, 1984]. We note that the predicted ratio V/W is very high. The disagreement could be attributed to the too early truncation of the elementary amplitude (only s and p waves) and to the use of the local t matrix at an energy which is too high [Niskanen, 1984].

Elastic scattering from ^7Li, ^{40}Ca and ^{208}Pb at 47 MeV, and ^{16}O and ^{18}O at 180 MeV have also been measured and are being analysed.

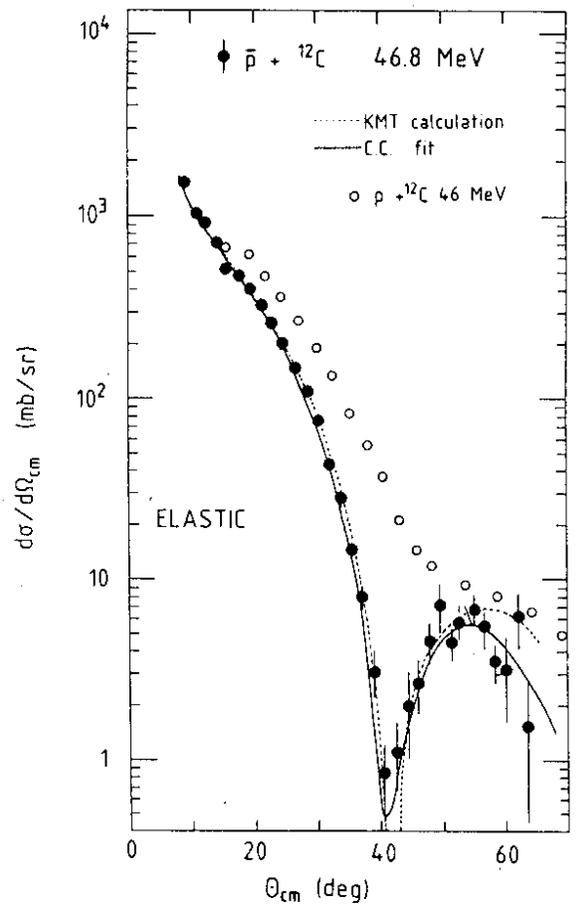

Fig. 3 Differential cross-sections for $\bar{p}$–elastic scattering from ^{12}C (solid circles). The cross-sections for proton elastic scattering are also shown for comparison (open circles). The dotted curve is a KMT calculation (see text) using $\bar{N}N$ amplitudes of Coté et al. [1982]. The solid curve results from a coupled-channel fit to the data with the following parameters: (V_0, W_0, r_{0v}, a_v, r_{0w}, a_w) = (25 MeV, 61 MeV, 1.17 fm, 0.61 fm, 1.2 fm, 0.51 fm).

Fig. 4 Differential cross-sections for $\bar{p}$–elastic scattering from ^{12}C, ^{40}Ca, and ^{208}Pb (solid circles). The cross-sections for proton elastic scattering are also shown for comparison (open circles). The dashed and dotted curves are KMT calculations (see text) using $\bar{N}N$ amplitudes of Dover and Richard [1982] and Coté et al. [1982], respectively. The solid curves result from an optical-model fit to the data (see text) with the following parameters: V_0 = 30 MeV, r_{0v} = 1.225 fm, and r_{0w} = 1.1 fm for all three targets, and W_0 = 118, 124, 172 MeV, a_v = 0.514, 0.572, 0.672 fm, and a_w = 0.500, 0.590, 0.649 fm for C, Ca, and Pb, respectively.

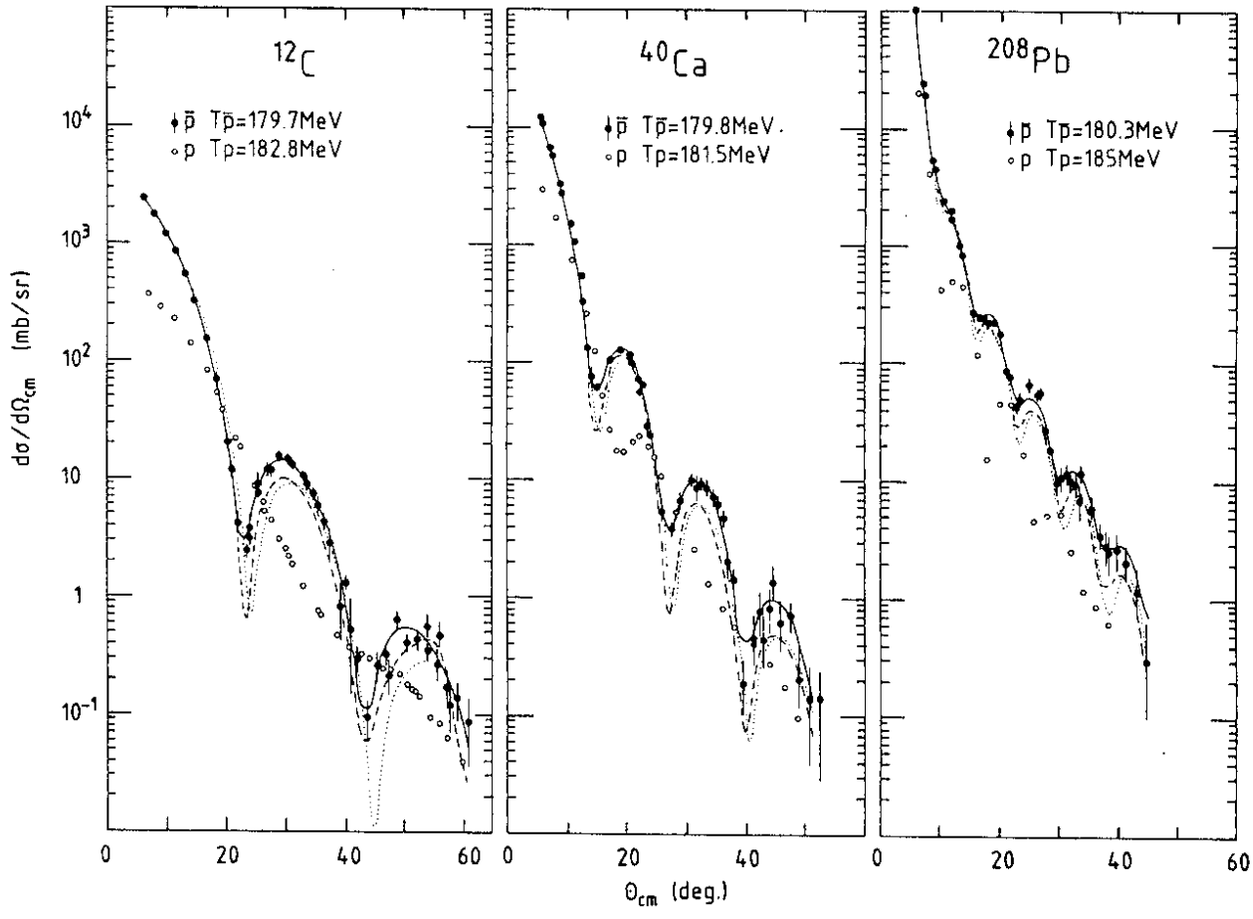

4. INELASTIC SCATTERING

Inelastic scattering angular distributions measured from ^{12}C at 46.8 MeV and 180 MeV are displayed in Fig. 5. For the 4.44 MeV, 2^+ state, it is clear that they are typical of a diffractional pattern, the oscillations being out of phase with those of the elastic scattering. Coupled channel calculations performed with the ECIS code reproduce well the data (solid curves) with deformation lengths β_{2N} R_{2N} with values extracted from proton inelastic scattering [Satchler, 1967]. At 46.8 MeV it was shown [Garreta et al., 1984a] that inelastic scattering sets further constraints on the determination of V_0 compared to what it is when using elastic scattering alone.

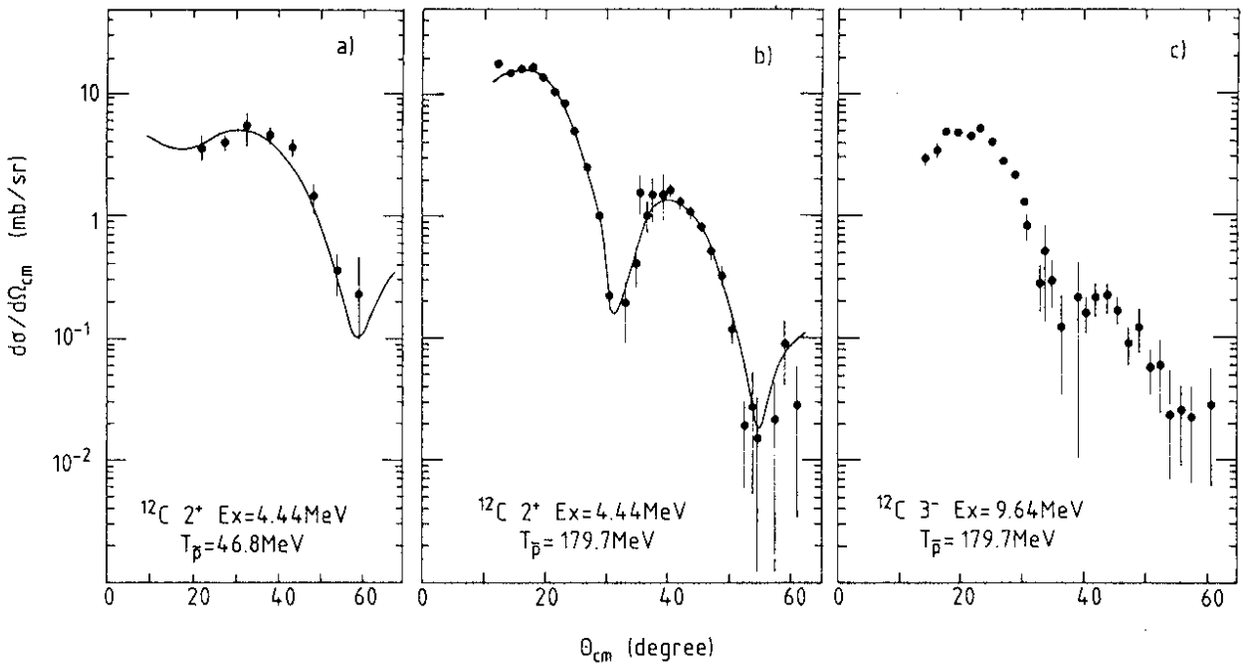

Fig. 5 Differential cross-section for $\bar{p}$ + ^{12}C inelastic scattering. In (a) each point corresponds to a measurement integrated over an angular range of 7.2°. In (b) and (c) the angular resolution is the same as for elastic scattering (see text). The solid curves result from a coupled channel fit to the data with the following parameters: (a) the optical-potential parameter are those of Fig. 3 and the deformation length β_{2N} R_{2N} = − 1.6 fm; (b) (V_0, W_0, r_{0v}, a_v, r_{0w}, a_w) = 40.7 MeV, 176 MeV, 1.116 fm, 0.522 fm, 1 fm, 0.487 fm) and β_{2N} R_{2N} = − 1.71 fm.

Inelastic scattering from the two 1^+ unnatural parity states of ^{12}C at 12.7 MeV (T = 0) and 15.1 MeV (T = 1) excitation energy have also been measured at 180 MeV at forward angle and are being analysed. These measurements are very important because it has been shown [Dover et al., 1984], that the corresponding cross-sections are very sensitive to the spin and isospin components of the elementary amplitudes. In particular, at 180 MeV and forward angle, the ratio between the cross-sections to the 12.7 MeV and 15.1 MeV states is predicted [Dover, 1984a] to be almost an order of magnitude larger with the Paris amplitudes than with the Dover and Richard amplitudes.

5. THE ($\bar{p}$,p) REACTION

Energy spectra of protons coming from scintillator, ^{12}C, ^{63}Cu and ^{209}Bi targets bombarded with the 180 MeV antiproton beam of LEAR are shown in Figs. 6 and 7 [Garreta et al., 1984c]. They are well reproduced (solid curves) by a Maxwellian distribution $d^2\sigma/d\Omega dE = C\sqrt{E}\exp(-E/T)$, where T is associated with an "effective temperature". The values of C and T which fit the data are given in Table 2. These energy spectra of protons emitted after antiproton annihilation in a nucleus have been calculated by several groups [Clover et al., 1982; Cahay et al., 1982 and 1983; Iljinov et al., 1982], using an intranuclear cascade (INC) model. In particular, Clover et al. have made the calculation for $\bar{p}$+ ^{12}C annihilation at 600 MeV/c. Their result, plotted as the dashed curve in Fig. 6b, is in good agreement with the data in the overall magnitude. However, the predicted slope is somewhat steeper than that of the data. This corresponds to the difference between the value of 62 MeV deduced from the calculation [Clover, 1982], and the measured value of 86 MeV. The nearly isotropic angular dependence in the $^{12}C(\bar{p},p)$ reaction is consistent with the cascade calculation. From the measured ($\bar{p}$,p)

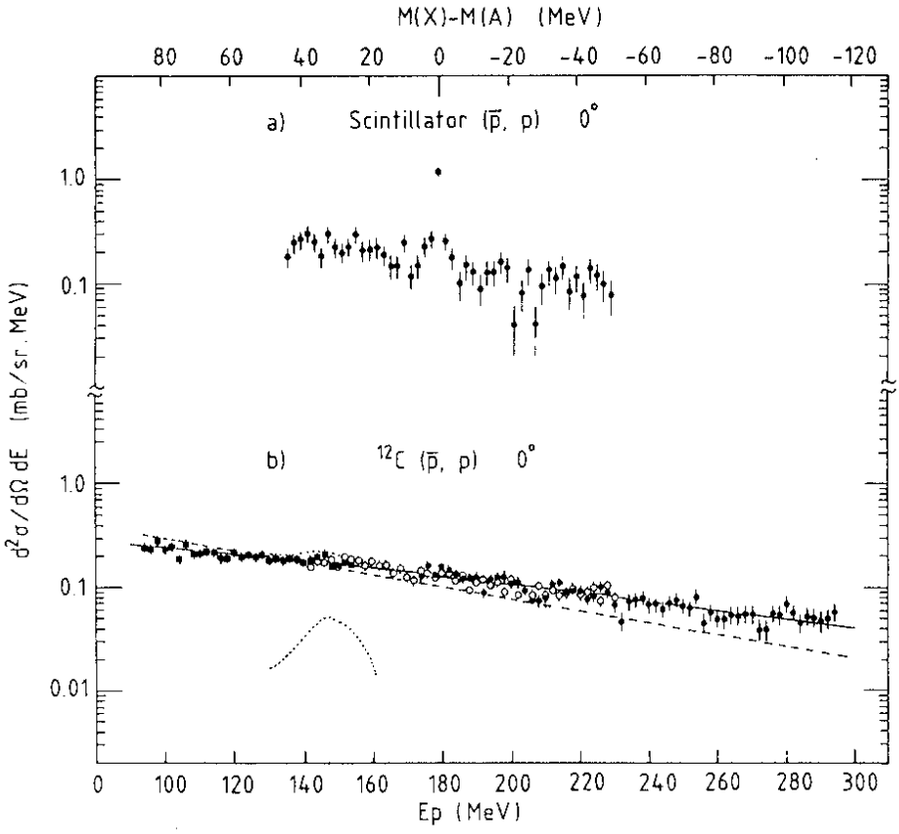

Fig. 6 Proton spectra for the A($\bar{p}$,p)X reaction at $T_{\bar{p}}$ = 180 MeV and 0° (a) for scintillator and (b) for carbon targets. The double differential cross-section is plotted versus the proton kinetic energy and the mass difference [M(X) − M(A)]. The sharp peak near 180 MeV in (a) corresponds to elastic scattering from hydrogen. Also shown are an INC calculation (dashed line) and a Maxwellian distribution best fit (solid line). A calculation for the quasi-free cross-section is indicated by the dotted curves.

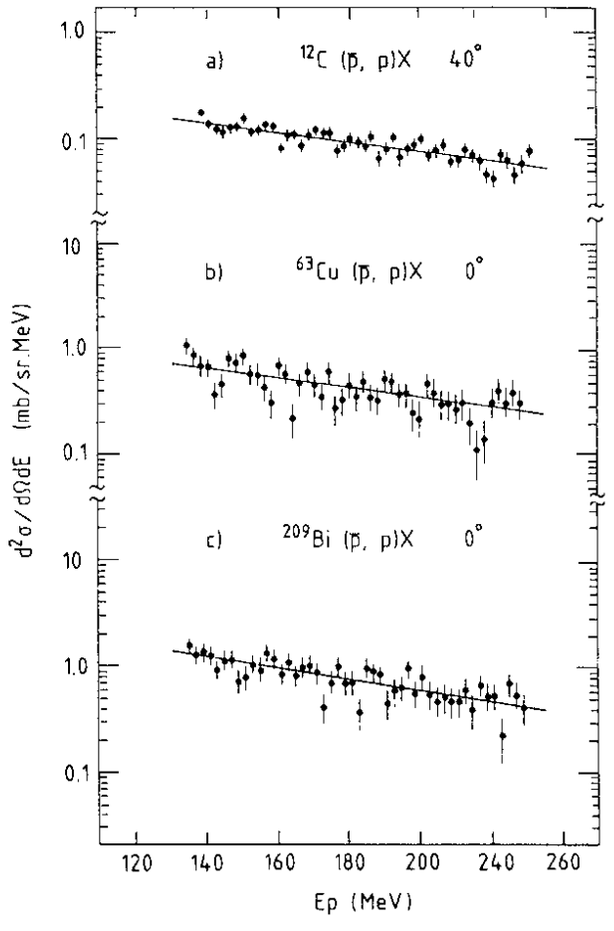

Fig. 7 The ($\bar{p}$,p) spectra from ^{12}C at 40°, and from ^{63}Cu and ^{209}Bi at 0°. The solid curves are best fits assuming a Maxwellian distribution.

Table 2
Parameters resulting from the best fits to the proton spectra with the expression
$d^2\sigma/d\Omega dE = C\sqrt{E}\exp(-E/T)$

Target	θ_{lab} (degrees)	T (MeV)	C (μb/sr · MeV$^{3/2}$)
^{12}C	0	86 ± 1.5	80
^{12}C	40	77 ± 6	75
^{63}Cu	0	69 ± 10	405
^{209}Bi	0	69 ± 7	770

cross-section for ^{12}C, ^{63}Cu and ^{209}Bi, at 180 MeV proton energy, we deduce a mass dependence $A^{0.63}$, in good agreement with the $A^{0.67}$ dependence we deduce from Clover et al. [1982]. The narrow peak observed in Fig. 1a near 180 MeV comes from the 180° $\bar{p}p$ elastic scattering. The sharpness of this peak reflects the good energy resolution (~ 1 MeV) in the present experiment. The c.m. cross-section of this reaction is measured to be 0.67 ± 0.10 mb/sr, in good agreement with a previous experiment [Alston-Garrjost et al., 1979]. We calculated semiclassically the cross-section of the quasi-free $p(\bar{p},p)\bar{p}$ reaction with protons of the target nucleus for the $p_{3/2}$ proton shell of ^{12}C assuming that ^{11}B recoils with momentum opposite to the Fermi momentum of the proton before collision. The shape of the momentum distribution of the proton was taken to be uniform sphere of k_F = 220 MeV/c [Moniz et al., 1971], and the effective number of $p_{3/2}$ shell protons contributing to the quasi-free process was estimated by Bouyssy [1984] to be 0.5. The calculated cross-section is shown by the dotted curve in Fig. 6b. The spectra of Figs. 6 and 7 offer no clear evidence of any peak which could be attributed to a $\bar{p}$–nucleus state. Although a direct comparison cannot be made with the calculation of Heiselberg et al. [1983], their prediction of a peak cross-section of 0.3 mb/sr · MeV for ^{16}O $(\bar{p},p)_{\bar{p}}{}^{15}N$ at $E\bar{p} \approx 100$ MeV appears to be too large and is not supported by the present measurement. But the statistics of the present measurements are rather poor. Measurements from ^6Li and scintillator targets have been performed with higher statistics and are being analysed.

6. CONCLUSIONS

We have found that the real and imaginary potentials are well determined by elastic scattering only at the nuclear surface, where $|W(R)| \gtrsim 2|V(R)|$. If we assume a Woods-Saxon geometry the real potential is found to be attractive but shallow. If the geometry is derived from that of the charge distribution, V_0 and W_0 are well determined, with $V_0 < 70$ MeV and $W_0 > 2\ V_0$. These results indicate that the surface of the nucleus is not transparent to antiprotons up to 180 MeV, even though 180 MeV antiprotons seem to probe the nucleus more deeply than 46.8 MeV ones. Our results do not support the orbiting idea [Auerbach et al., 1981; Kahana and Sainio, 1984], the relativistic mean field approach [Bouyssy and Marcos, 1982], and one microscopic calculation [Niskanen and Green, 1983; Niskanen, 1984]; they agree with the conclusions of Batty et al. [1984], that shallow imaginary potentials should be ruled out, and are in fair agreement with several microscopic calculations. Comparison of elastic scattering from ^{16}O and ^{18}O should be a sensitive test of the $\bar{p}n$ elementary amplitude. Inelastic scattering from collective states sets further constraints on the determination of the optical potential. Inelastic scattering from unnatural parity states will be a powerful test of the elementary $\bar{N}N$ amplitudes.

We have also reported the results of the first $(\bar{p},p)$ experiment intended to search for $\bar{p}$–nucleus states. No evidence of such states has been observed in the present experiment. Further measurements with improved statistics will provide more sensitive limits on the cross-sections of such states. The gross features in the $(\bar{p},p)$ spectra can be explained by INC calculations. Protons emitted after antiproton annihilation are a major source of "background", which complicates the task of finding $\bar{p}$–nucleus states. These background protons will be less abundant with lighter target nuclei such as ^3He and ^6Li, because of the A dependence of the emission cross-section. Other reactions such as $A(\bar{p},\Lambda)_{\bar{\Lambda}}(A-1)$ could also be contemplated [Peng, 1983; Dover, 1984b] since the cascade background would be absent. Unfortunately the cross-section of the $p(\bar{p},\Lambda)\bar{\Lambda}$ reaction is small. Finally, one could also consider detecting $\bar{p}$-nucleus resonant states [Auerbach, 1981] by measuring excitation functions of the $(\bar{p},\bar{p})$ or $(\bar{p},\bar{p}')$ reactions. Further experimental efforts are definitely required in order to search for $\bar{p}$-nucleus states.

7. REFERENCES

Agnew L E et al. 1957 Phys. Rev. **108** 1545

Aihara H et al. 1981 Nucl. Phys. **A360** 291 and references therein

Alston-Garrjost et al. 1979 Phys. Rev. Lett. **43** 1901

Auerbach E H, Dover C B and Kahana S 1981 Phys. Rev. Lett. **46** 702

Barrett R C and Jackson D F 1977 Nuclear sizes and structure (Oxford: Clarendon Press) p. 263

Batty C J 1981 Nucl. Phys. **A372** 433 and references therein

Batty C J, Friedman E and Lichtenstadt J 1984 Optical potentials for low-energy antiproton-nucleus interactions, Rutherford Appleton Laboratory, Didcot

Bouyssy A and Marcos S 1982 Phys. Rev. Lett. **114B** 397

Bouyssy A 1984 Private communication

Bruge G 1984 report DPh-N Saclay No. 2136

Cahay M, Cugnon J, Jasselette P and Vandermeulen J 1982 Phys. Lett **115B** 7

Cahay M, Cugnon J and Vandermeulen J 1983 Nucl. Phys. **A393** 237

Chaminade R, Durand J M, Faivre J C and Pain J 1974 Nucl. Instrum. Methods **118**, 477

Clover M R, De Vries R M, DiGiacomo N J and Yariv Y 1982 Phys. Rev. C **26** 2138

Coté J et al. 1982 Phys. Rev. Lett. **48** 1319

Dalkarov O D and Karmanov V A 1984 Lebedev Inst. preprint No. **77**

Dover C B 1984a Private communication

Dover C B 1984b Proc. 10th Int. Conf. on Few Body Problems in Physics Karlsruhe 1983 (Amsterdam: North Holland) vol. 1

Dover C B, Gal A and Richard J M 1983 Phys. Rev. **D** 27 1090

Dover C B and Richard J M 1982 Phys. Rev. C 25 1252

Dover C B et al. 1984 Antinucleon-nucleus inelastic scattering and the spin dependence of the $\bar{N}N$ annihilation potential, Orsay preprint IPN

Garreta D et al. 1984a Phys. Lett. **135B** 266, and **139B** 464

Garreta D et al. 1984b Preprint CERN-EP/84-93

Garreta D et al. 1984c Preprint CERN-EP/84-92

Green A M and Wyceh S 1982 Nucl. Phys. **A377** 441

Heiselberg H, Jensen A S, Miranda A and Oades G C 1983 Phys. Lett **132B** 279

Iljinov A S, Nazaruk V I and Chigrinov S E 1982 Nucl. Phys. **A382** 378

Kahana S H and Sainio M E 1984 Phys. Lett. **139B** 231

MacKellar A D, Satchler G R and Wong C Y 1984 Z. Phys. **A316** 35

Moniz E J et al. 1971 Phys. Rev. Lett. **26** 445

Nakamura K et al. 1984 Phys. Rev. Lett. 52 731

Niskanen J A 1984 Private communication

Niskanen J A and Green A M 1983 Nucl. Phys. **A404** 495

Peng J C 1983 Proc. 3rd LAMPF II Workshop, Los Alamos, July 1983, Report LA-9933-C, p. 531

Raynal J 1981 Phys. Rev. C 23 2571

Sakitt M 1984, paper presented at this conference

Satchler G R 1967 Nucl. Phys. **A100** 497

Thirion J and Birien P Le spectromètre SPES II, Rapport DPHN/ME, Saclay

Von Geramb H V 1979 Microscopic Optical Potentials, Hamburg, 1978, Lecture Notes in Physics (Berlin: Springer Verlag) vol. 89

Von Geramb H V, Nakano K and Rikus L 1984 Microscopic analysis of antiproton scattering from carbon, Universität Hamburg

Wong C Y, Kerman A K, Satchler G R and MacKellar A D 1984 Phys. Rev C 29 574